Depolarization of the supercontinuum induced by linearly and circularly polarized femtosecond laser pulses in water

Jing Li,[1] Wenjiang Tan,[1,*] Jinhai Si,[1] Shiyun Tang,[1] Yang Yang,[2] and Xun Hou[1]

[1]*Key Laboratory for Physical Electronics and Devices of the Ministry of Education, Shaanxi Key Lab of Information Photonic Technique, School of Electronic Science and Engineering, Xi'an Jiaotong University, Xi'an, ShaanXi 710049, China*

[2]*Department of Material Chemistry, Graduate School of Engineering, Kyoto University, Kyoto 615-8510, Japan*

(Received 13 August 2021; accepted 18 November 2021; published 30 November 2021)

The supercontinuum (SC) is generally assumed to inherit the polarization of the incident pulse in isotropic media. In this study, we experimentally investigated the polarization properties of SC spectra induced by different polarized femtosecond lasers in water. The results show that the extent of depolarization of the SC induced by a quasicircularly polarized pulse is more pronounced than that of a quasilinearly polarized pulse. In terms of the different spectral components, the long-wavelength components experienced more depolarization, and the short-wavelength components tended to be linearly polarized for both polarized input femtosecond lasers. The depolarization mechanism can be attributed to two factors, namely, the energy coupling between the two polarized components of the input femtosecond pulse, and the various degrees of nonlinear birefringence experienced by different spectral components of the SC during propagation.

DOI: 10.1103/PhysRevA.104.053535

I. INTRODUCTION

The propagation of intense femtosecond laser pulses in transparent media is accompanied by a series of phenomena such as filamentation, terahertz radiation, supercontinuum (SC) spectrum generation, and conical emission. The process of SC generation was first discovered by Alfano and Shapiro in 1970 [1]. The underlying physics of SC generation is generally complex as it involves several nonlinear processes that include self-phase modulation (SPM) [2], self-steepening [3,4], multiphoton ionization (MPI) [5], space-time focusing [6], four-wave mixing, and phase matching "scattering" [7,8]. In addition to these mechanisms, chromatic dispersion also plays a role in SC generation [9]. SC generation has attracted great interest in the fields of science and technology. SC represents a unique source of ultrabroadband radiation with high spectral brightness and a high degree of spatial coherence, equivalent to a white-light laser. SC has found numerous applications including pulse compression [10], time-resolved spectroscopy [11], dense wavelength division multiplexing [12], biomedical imaging [13], and detection of pollutants using broadband spectrum light detection and ranging (LIDAR) [14].

The polarization characteristics of SCs have considerable potential for applications in remote sensing and time-resolved spectroscopy. Earlier research confirmed that the generation of SC depends on the polarization of the incident laser; the SC was suppressed by circularly polarized light [15]. Further research indicated that increasing the ellipticity of the incident laser polarization with increasing ellipticity was caused by the suppression of SC generation, which was independent of the nature of the sample [16]. Most studies have focused on the laser polarization effect on the spectral intensity and spectral bandwidth of the SC [17–19]. However, few studies have investigated the polarization properties of SCs. The polarization of the SC is closely related to the polarization state of the incident pulse. It is generally considered to follow the state of polarization of the input pump pulse in an isotropic medium [2]. For instance, Kartazaev and Alfano reported that the polarization of the SC generated in fused silica and BK7 glass was the same as that of the pump light [20]. Midorikawa *et al.* observed that the polarization of the SC generated from water and fused silica was almost the same as that of the incident beam [21]. De Boni *et al.* reported that picosecond pulses induced SC in water preserved the polarization state of the incident beam within this temporal regime [22]. However, some researchers disagree with the above findings [23,24]; they found that the extinction ratio of the white-light spectra generated in BK7 experienced depolarization at higher intensities. The depolarization was because of the contribution of free electrons generated by MPI. In addition, Yu *et al.* reported that the depolarization of white light depended greatly on the initial polarization perturbation induced by the focus lens [25]. However, most previous studies on the polarization properties of SCs predominantly used linearly polarized incident pulses.

In this work, we studied the depolarization of SCs induced by different polarized femtosecond lasers. The polarization properties of all the spectral components of the SC were analyzed. Our results showed that when the initial pulse underwent a small perturbation, the depolarization of the SC was amplified by the nonlinear propagation of the femtosecond laser. The SC spectrum maintained nearly the same polarization for linearly polarized input femtosecond pulses but experienced more depolarization for circularly polarized input femtosecond pulses. The depolarization of the short-wavelength components of the SC was more pronounced

*Corresponding address: tanwenjiang@mail.xjtu.edu.cn

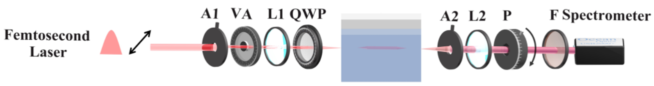

FIG. 1. Experimental setup. A: aperture; VA: variable attenuator; L: lens; QWP: quarter-wave plate; P: polarizer; F: filter.

than that of the long-wavelength components for a circularly polarized pulse. The extent of depolarization of the SC induced by a quasicircularly polarized pulse is more pronounced than that of a quasilinearly polarized pulse. The variation of the polarization state, originating from the energy coupling between the two circularly polarized components of the input femtosecond pulse and the influence of nonlinear birefringence on the different spectral components, was proposed to explain the depolarization of SC.

II. EXPERIMENTAL SETUP

The experimental setup is schematically depicted in Fig. 1. A Ti: sapphire femtosecond laser system (Libra-USP-HE, Coherent Inc., USA) operating with a pulse duration of 50 fs and central wavelength of 800 nm at a repetition rate of 1 kHz was used in our experiment. The input pulse was horizontally polarized after the polarizer (PGT5012, Union Optic). The SC spectrum induced by a single filament has been widely used in various fields due to its good stability. Therefore, the SC spectrum in this paper was induced by a single filament. When the pulse energy was slightly above the self-focusing threshold, a single filament was obtained by regulating the laser beam using a variable attenuator and an aperture simultaneously. The average power of the input laser was approximately 1.2 mW, which could form a single filament in water for both linear polarization and circular polarization light. The maximum blueshift cutoff wavelength of the SC spectrum remained constant over a certain range of incident laser energies because of the intensity clamping effect. Hence, there is little effect on the polarization properties of SC with the same incident power. The SC intensity induced by the linear polarization beam was stronger as compared with the circular polarization beam at the same average power, which was explained by the higher threshold for self-focusing by the circular polarization beam than that by the linear polarization beam. The laser beam was then focused by a convex lens with a focal length of 150 mm into a cuvette filled with de-ionized water. Different polarization states of the input beam can be obtained by rotating a quarter-wave plate (WPZ4325-800, Union Optic). The SC is obtained by eliminating conical emission with the aid of an aperture after the cuvette. The SC spectra were recorded using a fiber-coupled spectrometer (USB2000+, Ocean Optics). The 800-nm fundamental frequency light was filtered out by a 700-nm short-pass filter (FESH0700, Thorlabs), thus limiting the range of the SC to the visible region (400–700 nm). A polarizer (PGT5012, Union Optic) was used to analyze the output polarization of the SC.

III. RESULTS AND DISCUSSION

We first studied the relationship between the polarization of the input laser and the polarization property of the SC. Two typical polarized input lasers were selected, i.e., a linearly polarized and a circularly polarized laser. A quarter-wave plate was used to adjust the polarization of the input laser and was placed after the lens to avoid the depolarization induced by the lens [25]. The polarization of the different spectral components of the photoinduced SC was quantified by the degree of polarization (DOP), which is defined by Eq. (1) [26,27]:

$$P(\lambda) = \frac{I_{\max}(\lambda) - I_{\min}(\lambda)}{I_{\max}(\lambda) + I_{\min}(\lambda)}. \tag{1}$$

When the polarization analyzer revolves by a cycle in 5° increments, the spectral data are recorded. $I_{\max}$ and $I_{\min}$ are the intensities detected as a function of wavelength. The integrated DOP can be obtained by calculating the integrated intensity of the entire spectra. Thus, the value of the DOP is equal to 0 for perfectly circular polarization, and the value is 1 for perfectly linear polarization.

The fast axis of the quarter-wave plate was first adjusted in the same direction as the input polarization to maintain linear polarization of the laser output from the femtosecond laser system. The DOP of the incident pulse after passing through the quarter-wave plate was approximately 0.99 in our experiment. The intensity variation of the SC spectrum under different analyzer angles is shown in Figs. 2(a) and 2(b). As shown in Fig. 2(a), the intensity of the SC spectrum gradually decreases as the analyzer angle varies from 0° to 90° and increases as the analyzer angle varies from 100° to 180°. When the polarizer angle was 90°, the intensity of the SC spectrum at different wavelengths was zero. The total intensity of the SC spectrum exhibited periodic variations with changing polarizer angle. The integrated intensity variation of the SC spectrum with the analyzer angle was then calculated and shown in Fig. 2(b). Triangles indicate the experimental data and the solid line is fitted by the Malus law [28]. It is observed that the variation of integrated intensity is in good agreement with the Malus law. The integrated DOP of the SC was calculated to be approximately 0.97. The results show that the SC was linearly polarized and maintained the same polarization as the input laser.

The incident pulse was then adjusted to be circularly polarized; the DOP of the incident pulse after passing through the quarter-wave plate was approximately 0.01, which was nearly circularly polarized. The intensity variation of the SC spectrum with the polarizer angle is shown in Figs. 2(c) and 2(d). It is believed that the polarization of the SC is the same as the input pulse in previous studies. This means that the SC spectrum intensity does not vary with the polarizer angle for a perfect circular polarization. However, the intensities of SC spectral components change with the analyzer angles in our experiment, as shown in Fig. 2(c). In Fig. 2(d), the circles represent the integrated intensity of the SC in the experiment and the solid line indicates the fitted curve by elliptical polarization at different analyzer angles. The elliptical azimuth (φ) obtained by fitting is 160°. It is observed that the calculation results agree well with the experimental data. Consequently, the polarization of the SC induced by a nearly circularly polarized incident femtosecond laser was neither circularly nor linearly polarized, but elliptically polarized. The integrated DOP of the SC was calculated to be approximately 0.12.

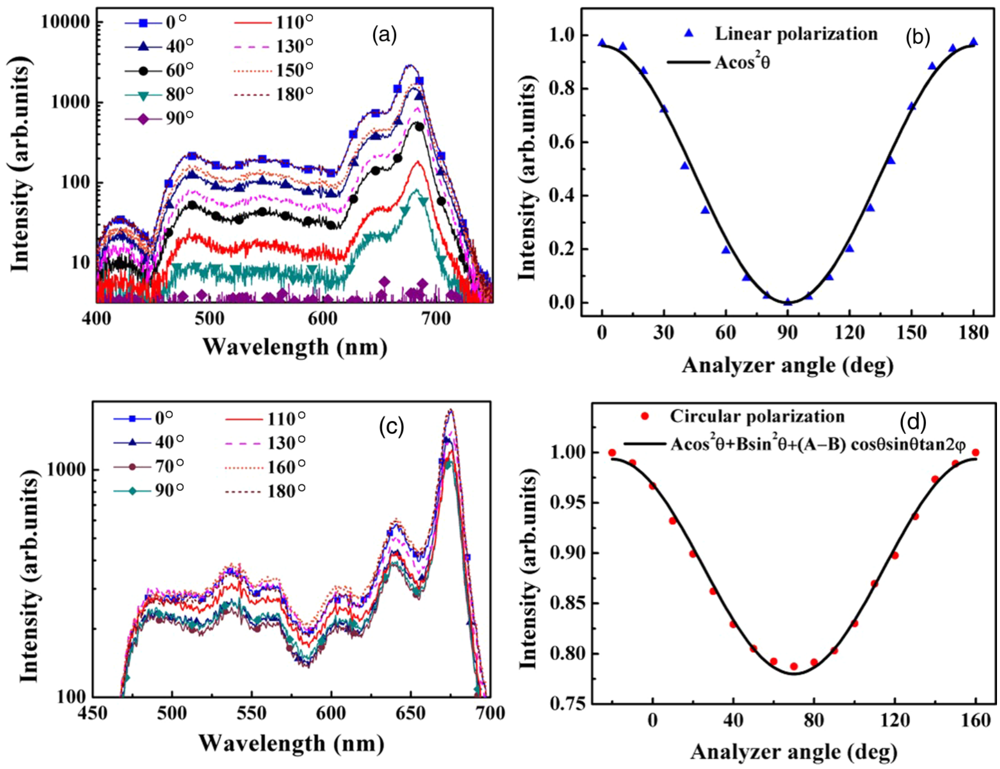

FIG. 2. Variation of the SC spectrum with different analyzer angles. (a) Overall spectrum and (b) integrated intensity of SC spectrum as a function of analyzer angles for linearly polarized input beam. (c) Overall spectrum and (d) integrated intensity of SC spectrum as a function of analyzer angles for circularly polarized input beam. Solid lines in (b), (d) are the fitting curves.

The results show that the SC experienced a certain degree of depolarization in this scenario.

The DOPs of all the spectral components of the SC were further analyzed, and the results are shown in Fig. 3. When the input femtosecond laser pulse was linearly polarized, the DOP values were close to 1 for all the spectral components, which indicates that the SC retained a good linear polarization characteristic for the linearly polarized input femtosecond laser. However, in the case of the circularly polarized input femtosecond laser, the DOP values for all the spectral components were greater than 0.08. This result shows that the SC has experienced a large degree of depolarization into elliptical polarization for a circularly polarized input femtosecond laser. We found that the DOP has obvious fluctuations in the range of 630 to 700 nm. This might be due to the intensity fluctuations of the high-intensity long-wavelength components of the SC and the Raman effect of the water [29].

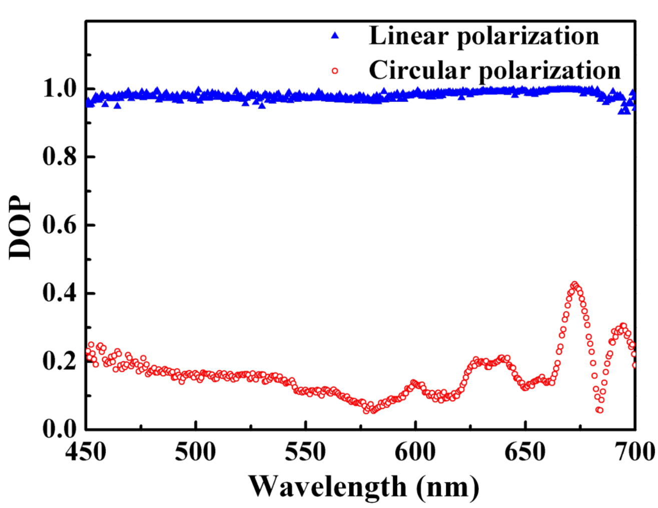

FIG. 3. Degree of polarization over the entire SC spectra for linearly and circularly polarized input beam.

When the incident pulse is not perfectly circularly polarized, the depolarization of the SC can be attributed to the amplification of the polarization perturbation in the incident pulse during its nonlinear propagation. We further analyzed the polarization properties of the SC with different polarized input femtosecond lasers. Two typical sets of elliptically polarized input light with different DOPs were artificially generated. The DOPs of the SC spectra generated by four different quasilinear polarization states were compared. As shown in Fig. 4(a), there is a larger depolarization effect in the long-wavelength direction of the SC spectra for a quasilinearly polarized incident laser. The values of the DOP gradually increase toward the short-wavelength direction of the SC spectra in the range of 625–450 nm. For some short-wavelength components, the values approach 1, which illustrates that these spectral components tend toward linear polarization. For example, when the DOP of the input pulse was 0.93, all the spectral components were depolarized relative to the input pulse. The DOPs of the spectral components were greater than 0.93 at wavelengths ranging from 450 to 600 nm and exhibited nearly linear polarization. When the input pulse was quasicircularly polarized, the DOP of the SC

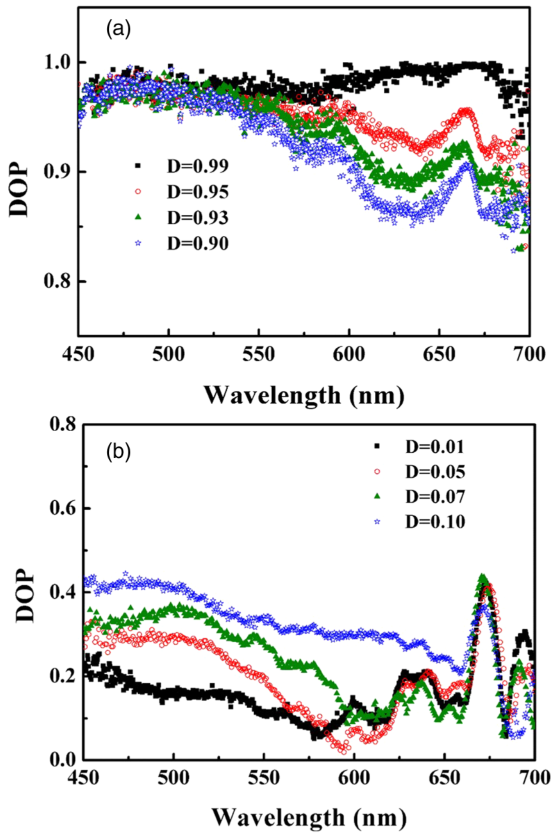

FIG. 4. DOP of the SC spectrum at different incident pulse disturbance. (a) Quasilinearly polarized input laser; (b) quasicircularly polarized input laser.

spectra was measured, as shown in Fig. 4(b). It is obvious from Fig. 4(b) that the DOPs of the SC spectra are different from those of the incident laser. The DOPs of the SC spectra also gradually increased with the decreasing wavelength of the SC spectral components in the range of 625–450 nm. This indicates that the short-wavelength components experience considerable depolarization. The common feature is that there is a peak around 670 nm, which implies a large depolarization in the long-wavelength components. In addition, for both quasilinearly and quasicircularly polarized input femtosecond laser, the SC spectra experience more depolarization with increasing polarization perturbation of the incident pulse.

The results shown in Fig. 4 suggest that the depolarization of the different spectral components of the SC would be amplified for different polarized input femtosecond lasers if the input pulse is slightly perturbed. Moreover, the DOPs of all the spectral components of the SC gradually increase with decreasing wavelength. This phenomenon aids the SC induced by a linearly or quasilinearly polarized input femtosecond laser to maintain the same linear polarization. However, the SC induced by a circularly or quasicircularly polarized input femtosecond laser suffers from a more pronounced depolarization.

According to previous studies, different spectral components of the SC are generated at different positions during the laser pulse propagation [30]. The leading edge of the pulses interacting with the medium mainly contributes to the long-wavelength components of the SC. The short-wavelength components are generated by the tailing edge of the pulses. We attribute the depolarization properties of the SC spectrum to the polarization evolution of the input femtosecond pulse and the influence of the nonlinear birefringence on different spectral components. The detailed explanations are given below.

When polarized light propagates in an isotropic medium, it is convenient to divide the optical electric field into the right-handed circularly polarized component (E^+) and the left-handed circularly polarized component (E^-). The propagation of the ultrashort pulse in the medium can be described by the coupled nonlinear Schrödinger equation, as expressed by Eqs. (2) and (3). The equations take into account the effects of diffraction, normal group-velocity dispersion, multiphoton ionization, self-focusing and plasma defocus, and cubic nonlinearity in combination.

$$\begin{aligned}\frac{\partial E^+}{\partial z} &= \frac{i}{2k}\nabla_\perp^2 E^+ - \frac{ik''}{2}\frac{\partial^2 E^+}{\partial t^2}\\ &\quad - \frac{\sigma}{2}(1+i\omega\tau)\rho E^+ - \frac{\beta^{(K)}}{2}|E|^{2K-2}E^+\\ &\quad + \frac{2i\omega}{3c}n_2|E^+|^2E^+ + \frac{4i\omega}{3c}n_2|E^-|^2E^+, \qquad (2)\end{aligned}$$

$$\begin{aligned}\frac{\partial E^-}{\partial z} &= \frac{i}{2k}\nabla_\perp^2 E^- - \frac{ik''}{2}\frac{\partial^2 E^-}{\partial t^2}\\ &\quad - \frac{\sigma}{2}(1+i\omega\tau)\rho E^- - \frac{\beta^{(K)}}{2}|E|^{2K-2}E^-\\ &\quad + \frac{2i\omega}{3c}n_2|E^-|^2E^- + \frac{4i\omega}{3c}n_2|E^+|^2E^-. \qquad (3)\end{aligned}$$

Here, $|E|^2 = |E^+|^2 + |E^-|^2$; the coefficient of group-velocity dispersion is $k'' = \partial^2 k/\partial\omega^2$, $k = n_0\omega/c$. The cross section for inverse bremsstrahlung is $\sigma = ke^2\tau/\omega m_e\varepsilon_0[1+(\omega\tau)^2]$, ω is the optical frequency, ρ is the electron density, n_2 is the nonlinear index, n_0 is refractive index of water, τ is the electron collision time, K is the number of photons at the frequency ω, and $\beta^{(K)}$ corresponds to the K-photon absorption coefficient.

In this study, we assumed that the right-handed circularly polarized component (E^+) was greater than the left-handed circularly polarized component (E^-) for elliptic polarization. We call E^+ the strong component, and E^- the weak component. When the input pulse was quasilinearly polarized, E^- was slightly less than E^+. However, E^- was far less than E^+ for quasicircularly polarized incident femtosecond lasers. It can be seen from the sixth term of the equations that the two circularly polarized components are coupled owing to cross-phase modulation. The energy redistribution between the right- and left-handed circularly polarized components was investigated by simulation, as shown in Fig. 5. The numerical parameters for the simulation are listed in Table I. As the figure shows, the propagation distance was measured from the focusing lens; the geometrical focus was located at position 0. It was observed that the self-focusing event occurred at 250 μm before the geometric focus. The simulation result indicates that the energy exchange between the two polarized components begins at the self-focusing position and increases

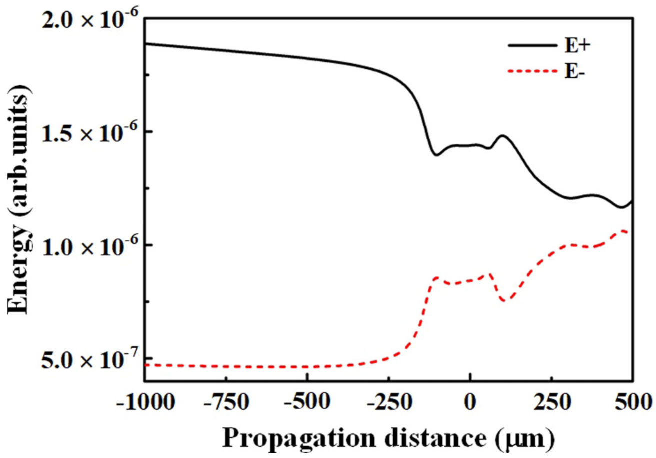

FIG. 5. Variation of the right- and left-handed polarized components with propagation.

with the propagation distance. The stronger polarized component transfers energy into the weaker one, resulting in a trend toward equality.

The energy transfer between the polarization components was analyzed in detail. When the linearly polarized input pulse experiences a slight depolarization, less energy transfer between the two circularly polarized components is required to restore its polarization to a linearly polarized state. When the input femtosecond pulse propagated to a certain location in the medium, the generation of short-wavelength components of the SC always lagged behind that of the long-wavelength components. Therefore, the extent of the linear polarization restoration was more intense for the short-wavelength components, as shown in Fig. 4(a). In the case of a circularly polarized input pulse with slight depolarization, the energy transfer further increased its depolarization, thereby contributing to more intense depolarization in the short-wavelength components, as shown in Fig. 4(b). Moreover, the nonlinear refractive index of the two circularly polarized components of the beam in the medium is given by

$$\triangle n_{\pm} = 2\pi [A(|E_{\pm}|^2 + |E_{\mp}|^2) + B|E_{\mp}|^2]/n_0. \qquad (4)$$

For a perfectly linearly polarized pulse, the change in the refractive index calculated was 0. For a perfectly circularly polarized pulse, there was only one circularly polarized component. This implies that there was no energy transfer during the propagation in the medium. The polarization properties of the input pulse were well maintained for perfectly linearly and circularly polarized pulses.

The nonlinear birefringence also had a major impact on the depolarization of the SC. Essentially, the effect of nonlinear birefringence on the different spectral components depended strongly on the group-velocity dispersion. The temporal walk-off between different wavelengths is related by Eq. (5), where v_g is group velocity and n_g the group refractive index. The group velocity of the long-wavelength components of the SC is close to that of the input fundamental frequency light; therefore, they experienced more depolarization owing to the significant influence of the birefringence induced by the fundamental frequency light. However, the group velocity of the short-wavelength components of the SC is less than that of the input fundamental frequency light. Correspondingly, the short-wavelength components were affected by the walk-off phenomena and had less depolarization. For instance, the temporal walk-off is approximately 80 fs between the wavelengths 480 and 680 nm, which is larger than a pulse duration. It means that the wavelength of 480 nm is less influenced by the birefringence. The overall depolarization of the SC was increased during nonlinear propagation.

$$\Delta t = z\left[\frac{1}{v_g(\lambda_i)} - \frac{1}{v_g(\lambda_k)}\right] = \frac{z}{c}[n_g(\lambda_i) - n_g(\lambda_k)]. \qquad (5)$$

In general, the influence of the input pulse polarization and nonlinear birefringence should be considered in the depolarization of the SC spectrum. As discussed above, the energy redistribution between two circularly polarized components accumulated as the pulse propagated. The short-wavelength components of the SC always exhibited a tendency toward linear polarization for both quasilinearly and quasicircularly polarized input pulses. This means that the SC will preserve linear polarization for quasilinearly polarized pulses more and experience more depolarization for quasicircularly polarized pulses. In addition, all the spectral components were further depolarized owing to the influence of nonlinear birefringence. The depolarization of the long-wavelength components was more pronounced than that of the short-wavelength components. In conclusion, our results indicated that SC experienced depolarization regardless of whether the input pulse was quasilinearly or quasicircularly polarized. Moreover, the depolarization of the SC induced by a quasicircularly polarized pulse is more pronounced than that induced by a quasilinearly polarized pulse.

It should be noted that there was no real comparison between the numerical model and experimental results mentioned above, because a more comprehensive numerical model should be created to perform this comparison. First, the new numerical model must contain the detailed information about the generation of the SC spectrum. However, it is very complicated to simulate SC generation with its exact spectral width and intensity of each spectral component. Second, the energy coupling of the input pulse during its propagation and the role of nonlinear birefringence also must be considered in the model. So in this paper, we just indirectly revealed the depolarization mechanism of the SC spectrum through the basic simulation model. Building a comprehensive model and doing

TABLE I. Parameters used in the simulation.

Parameters	Values	Symbol (units)
Wavelength	800	λ (nm)
Refractive index of water	1.33	n_0
Nonlinear index	4.1×10^{-20}	n_2 (m^2/W)
Dispersion coefficient	2.0×10^{-29}	k' (s^2/m)
Multiphoton ionization order	5	K
Multiphoton ionization rate	8.3×10^{-67}	$\beta^{(K)}$ (W^{1-K} m^{2K-3})
Electron collision time	10^{-15}	τ (s)

more detailed analysis about the depolarization phenomena of the SC is our ongoing work.

Lenses, mirrors, optical films, and other optical elements may slightly change the polarization of the incident beam. The polarization of the SC spectrum is crucial because of its potential applications in optical parametric amplification and time-resolved spectroscopy. Our research suggests that it is necessary to avoid the depolarization of the SC by reducing the polarization perturbation of the incident light, especially for a circularly polarized input femtosecond laser pulse. Taking effective measures such as using a Soleil-Babinet compensator can generate a perfectly circularly polarized incident beam and further suppress the depolarization of the SC.

IV. CONCLUSION

In summary, we investigated the polarization properties of SCs generated using different polarized input pulses. For a linearly polarized input pulse, the SC spectrum maintained its polarization well, such that each wavelength had good linear polarization characteristics. When the laser beam was imperfectly circularly polarized, the SC spectrum experienced depolarization and exhibited elliptic polarization. The depolarization arising from the imperfection of the input pulse has been increased by the nonlinear propagation of the femtosecond laser. Furthermore, the depolarization properties of SCs were studied when the input pulses were quasilinearly and quasicircularly polarized with perturbations. In either case, the long-wavelength components of the SC experienced depolarization, and the short-wavelength components tended to be linearly polarized. Therefore, the SC has experienced less depolarization and retained the initial polarized state for a quasilinearly polarized input femtosecond laser. However, for a quasicircularly input femtosecond laser, the SC has exhibited more depolarization and significantly differs from the initial polarized state. The physical mechanism of depolarization was attributed to the energy coupling between the two polarized components of the input femtosecond pulse and the influence of nonlinear birefringence on the different spectral components. The result can be used for the application of white light as a coherent light source with explicit polarization properties.

ACKNOWLEDGMENTS

The authors gratefully acknowledge the financial support for this work provided by the National Natural Science Foundation of China (Grants No. 62027822 and No. 61690221), the National Key Research and Development Program of China (Grant No. 2019YFA0706402), the Natural Science Basic Research Plan in Shaanxi Province of China (Grant No. 2018JM6012), and Fundamental Research Funds for the Central Universities (Grant No. xzy012019039).

[1] R. R. Alfano and S. L. Shapiro, Emission in Region 4000 to 7000 Å via Four-Photon Coupling in Glass, Phys. Rev. Lett. **24**, 584 (1970).

[2] R. R. Alfano, *The Supercontinuum Laser Source: Fundamentals with Updated References*, 2nd ed. (Springer, Berlin, 2006).

[3] A. L. Gaeta, Catastrophic Collapse of Ultrashort Pulses, Phys. Rev. Lett. **84**, 3582 (2000).

[4] H. Ward and L. Bergé, Temporal shaping of Femtosecond Solitary Pulses in Photoionized Media, Phys. Rev. Lett. **90**, 053901 (2003).

[5] N. Bloembergen, The influence of electron plasma formation on superbroadening in light filaments, Opt. Commun. **8**, 285 (1973).

[6] J. E. Rothenberg, Space-time focusing: Breakdown of the slowly varying envelope approximation in the self-focusing of femtosecond pulses, Opt. Lett. **17**, 1340 (1992).

[7] M. Kolesik, E. M. Wright, and J. V. Moloney, Dynamic Nonlinear X Waves for Femtosecond Pulse Propagation in Water, Phys. Rev. Lett. **92**, 253901 (2004).

[8] M. Kolesik, E. M. Wright, and J. V. Moloney, Interpretation of the spectrally resolved far field of femtosecond pulses propagating in bulk nonlinear dispersive media, Opt. Express **13**, 10729 (2005).

[9] M. Kolesik, G. Katona, J. V. Moloney, and E. M. Wright, Theory and simulation of supercontinuum generation in transparent bulk media, Appl. Phys. B **77**, 185 (2003).

[10] E. T. J. Nibbering, O. Dühr, and G. Korn, Generation of intense tunable 20-fs pulses near 400 nm by use of a gas-filled hollow wave guide, Opt. Lett. **22**, 1335 (1997).

[11] J. Swartling, A. Bassi, C. D'Andrea, A. Pifferi, A. Torricelli, and R. Cubeddu, Dynamic time-resolved diffuse spectroscopy based on supercontinuum light pulses, Appl. Opt. **44**, 4684 (2005).

[12] H. Takara, T. Ohara, T. Yamamoto, H. Masuda, M. Abe, H. Takahashi, and T. Morioka, Field demonstration of over 1000-channel DWDM transmission with supercontinuum multi-carrier source, Electron. Lett. **41**, 270 (2005).

[13] C. Poudel and C. F. Kaminski, Supercontinuum radiation in fluorescence microscopy and biomedical imaging applications, J. Opt. Soc. Am. B **36**, A139 (2019).

[14] P. Rairoux, H. Schillinger, S. Niedermeier, M. Rodriguez, F. Ronneberger, R. Sauerbrey, B. Stein, D. Waite, C. Wedekind, H. Wille, L. Wöste, and C. Ziener, Remote sensing of the atmosphere using ultrashort laser pulses, Appl. Phys. B **71**, 573 (2000).

[15] A. S. Sandhu, S. Banerjee, and D. Goswami, Suppression of supercontinuum generation with circularly polarized light, Opt. Commun. **181**, 101 (2000).

[16] A. Srivastava and D. Goswami, Control of supercontinuum generation with polarization of incident laser pulses, Appl. Phys. B **77**, 325 (2003).

[17] N. Chen, T. J. Wang, Z. Zhu, H. Guo, Y. Liu, F. Yin, H. Sun, Y. Leng, and R. Li, Laser ellipticity-dependent supercontinuum generation by femtosecond laser filamentation in air, Opt. Lett. **45**, 4444 (2020).

[18] A. K. Dharmadhikari, S. Edward, J. A. Dharmadhikari, and D. Mathur, On the generation of polarization-dependent supercontinuum and third harmonic in air, J. Phys. B: At., Mol. Opt. Phys. **48**, 094012 (2015).

[19] Z. Shi, S. Li, H. Zhang, H. Li, X. Wang, A. Chen, and M. Jin, The dependence of external focusing geometries and polarization in generation of supercontinuum by femtosecond laser pulse in air, Optik **164**, 390 (2018).

[20] V. Kartazaev and R. R. Alfano, Polarization properties of SC generated in CaF_2, Opt. Commun. **281**, 463 (2008).

[21] K. Midorikawa, H. Kawano, A. Suda, C. Nagura, and M. Obara, Polarization properties of ultrafast white-light continuum generated in condensed media, Appl. Phys. Lett. **80**, 923 (2002).

[22] L. De Boni, C. Toro, and F. E. Hernández, Pump polarization-state preservation of picosecond generated white-light supercontinuum, Opt. Express **16**, 957 (2008).

[23] R. S. S. Kumar, K. L. N. Deepak, and D. N. Rao, Depolarization properties of the femtosecond supercontinuum generated in condensed media, Phys. Rev. A **78**, 043818 (2008).

[24] A. K. Dharmadhikari, F. A. Rajgara, and D. Mathur, Depolarization of white light generated by ultrashort laser pulses in optical media, Opt. Lett. **31**, 2184 (2006).

[25] J. Yu, H. Jiang, J. Wen, H. Yang, and Q. Gong, Mechanism of depolarization of white light generated by femtosecond laser pulse in water, Opt. Express **18**, 12581 (2010).

[26] W. Tao, H. Bao, and M. Gu, Enhanced two-channel nonlinear imaging by a highly polarized supercontinuum light source generated from a nonlinear photonic crystal fiber with two zero-dispersion wavelengths, J. Biomed. Opt. **16**, 056010 (2011).

[27] A. Saha, K. Bhattacharya, and A. K. Chakraborty, Depolarization of polarized polychromatic beam during propagation in a birefringent medium, Optik **127**, 5882 (2016).

[28] K. Wódkiewicz, Classical and quantum Malus laws, Phys. Rev. A **51**, 2785 (1995).

[29] D. Cavaille, D. Combes, and A. Zwick, Effect of high hydrostatic pressure and additives on the dynamics of water: A Raman spectroscopy study, J. Raman Spectrosc. **27**, 853 (1996).

[30] I. Buchvarov, A. Trifonov, and T. Fiebig, Toward an understanding of white-light generation in cubic media—polarization properties across the entire spectral range, Opt. Lett. **32**, 1539 (2007).